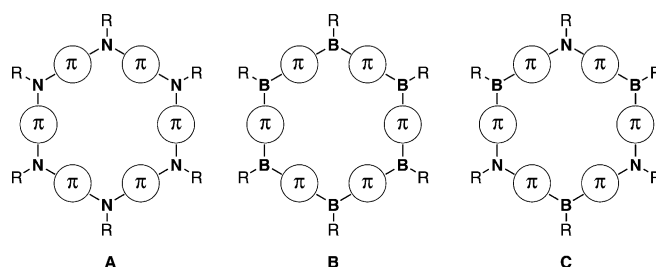


# $\pi$ -Expanded Borazine: An Ambipolar Conjugated B– $\pi$ –N Macrocycle\*\*

Pangkuan Chen, Roger A. Lalancette, and Frieder Jäkle\*

In reference to its isoelectronic and isostructural relationship with benzene, borazine is commonly referred to as “inorganic benzene”.<sup>[1]</sup> This concept has generated renewed interest in recent years, as the judicious replacement of C=C double bonds with isoelectronic and isosteric B–N fragments has resulted in a plethora of interesting molecules for applications ranging from hydrogen-storage materials to analogues of aromatic natural products, and new optical and electronic materials.<sup>[2–4]</sup> For instance, introduction of a B–N fragment in benzene results in polarization of the molecule, which in turn leads to unusual reactivity, including nucleophilic substitution and hydrogenation under mild conditions.<sup>[3,5]</sup> B–N functionalization of extended organic  $\pi$ -systems alters the electronic structure, resulting for example in low-lying LUMO levels and corresponding bathochromic shifts in the emission spectra.<sup>[4,6]</sup> In the previous examples, B and N are directly connected. An alternative design has borane acceptor (A) moieties separated from amine donors (D) by an organic  $\pi$ -conjugated linker. This D– $\pi$ –A approach has proven successful for the development of nonlinear optical materials, ambipolar charge carriers in organic light emitting devices (OLEDs), and fluorescent anion sensors.<sup>[7,8]</sup>

Conjugated macrocycles, on the other hand, are an attractive class of materials for optoelectronic applications as they comprise discrete, monodisperse structures, representative of an infinite polymer chain without any end groups.<sup>[9]</sup> Another interesting feature is their ability to self-assemble into tubular supramolecular structures and to form well-defined and highly symmetric arrays upon deposition on surfaces.<sup>[10]</sup> Numerous conjugated organic cyclic compounds have been explored. More recently, heteroatom-containing systems have attracted interest because the added functionality can offer unique properties and possibly open the door to new applications.<sup>[11,12]</sup> As an example, Tanaka’s cyclic hexaanilines **A** ( $\pi$  = phenylene) provide a platform for studies on the aromaticity and molecular magnetism that results from spin delocalization in the radical cation and dication.<sup>[11]</sup> We have introduced an electron-deficient charge-reverse analogue<sup>[13]</sup> to **A**, the conjugated macrocyclic organoborane **B** with fluorene as the  $\pi$ -system.<sup>[14]</sup> Herein, we report the first



ambipolar macrocycle, which contains nitrogen as donor and boron as acceptor sites, bridged by  $\pi$ -conjugated phenylene groups. This new type of macrocycle **C** may be viewed as a  $\pi$ -expanded borazine; however, introduction of the phenylene bridges results in remarkably different properties in comparison to borazine, including strong blue fluorescence, solvatochromic emission, and redox processes that reflect the ambipolar structure of this unique D– $\pi$ –A type macrocycle.

Initially, the linear oligomer **2-Si**, was prepared in 66% overall yield by Sn/B exchange of the stannyl group in **1-SiSn** with the boryl group in **1-SiB**, followed by treatment with triisopropylphenyl copper (TipCu) for steric protection of the boron center (Scheme 1). The selectivity of the Sn/B exchange relies on the much higher reactivity<sup>[15]</sup> of the Sn–C in comparison to the Si–C bond in **1-SiSn**. Formation of the ambipolar macrocycle **3** was accomplished by reaction of **2-Si**, with 2 equivalents BBr<sub>3</sub>, followed by cyclization under pseudo-high dilution conditions upon simultaneous addition of stoichiometric amounts of the resulting borylated species and **1-Sn** (1:1) to a large quantity of toluene. Treatment of the initially generated B–Br functionalized macrocycle with 2 equivalents of TipCu in refluxing toluene for 2 days gave the desired product **3**. GPC analysis indicated that the crude sample after standard workup consists of the targeted macrocycle as the major product in addition to a small amount of larger cyclic species and/or higher linear polymers.<sup>[16]</sup> Purification by preparative size exclusion column chromatography on Bio-beads with THF as the eluent gave analytically pure **3** as a pale yellow powdery solid in 38% overall yield over three steps.

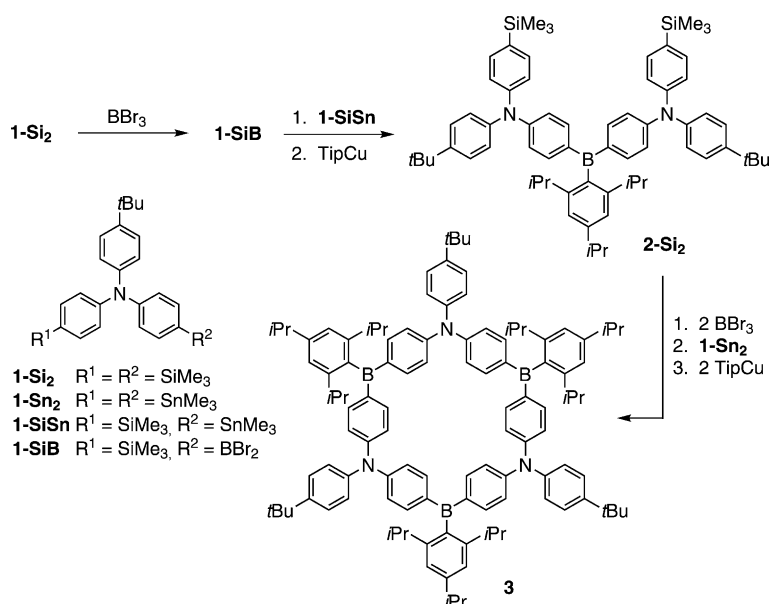
GPC analysis of purified **3** gave a single, monodisperse band corresponding to a molecular weight of  $M_n = 1483$  Da (polydispersity index (PDI) =  $M_w/M_n = 1.01$ ), which is close to the theoretical value of 1540 Da. Successful synthesis of the macrocyclic species was further confirmed by high-resolution MALDI-MS, which showed a single signal at  $m/z$  1540.0705 that can be assigned to the molecular ion peak (calcd 1540.0706).<sup>[16]</sup> Consistent with the highly symmetric cyclic structure, only one set of sharp signals was observed in the <sup>1</sup>H

[\*] P. Chen, Prof. Dr. R. A. Lalancette, Prof. Dr. F. Jäkle  
Department of Chemistry, Rutgers University, Newark  
73 Warren Street, Newark, NJ 07102 (USA)  
E-mail: fjaekle@rutgers.edu  
Homepage: <http://andromeda.rutgers.edu/~fjaekle>

[\*\*] This work is supported by the National Science Foundation under Grants No. CHE-0809642 and CHE-1112195.

Supporting information for this article is available on the WWW under <http://dx.doi.org/10.1002/anie.201203788>.





**Scheme 1.** Synthesis of the donor- $\pi$ -acceptor macrocycle **3**.

and <sup>13</sup>C NMR spectra, and a broad <sup>11</sup>B NMR resonance at  $\delta = 72$  ppm is indicative of tricoordinate B centers.<sup>[16]</sup>

Colorless hexagon-shaped single crystals that show blue fluorescence were obtained by slow vapor diffusion of dichloroethane into a solution of **3** in toluene (Figure 1). Compound **3** crystallizes in the trigonal space group  $R\bar{3}$  with eight molecules of dichloroethane per macrocycle for a total of six macrocycles and 48 solvent molecules per unit cell.<sup>[17]</sup> Due to the large size and exceedingly fast solvent evaporation from the crystals, and despite the use of dichloroethane in place of dichloromethane, the uncertainties are relatively large and only allow for a qualitative discussion. The

endocyclic B–C (1.546(6), 1.555(7) Å) and N–C (1.416(6), 1.432(6) Å) distances are similar to the exocyclic ones of 1.573(6) and 1.419(6) Å, respectively, and the endocyclic C–B–C (119.8(4)°) and C–N–C (121.3(3)°) angles are close to 120°, indicating that the ring system is not significantly strained. However, as evident from the side view in Figure 1b, rather than adopting perfect  $D_3$  symmetry, the B<sub>3</sub>N<sub>3</sub> core is distorted towards a chair-like conformation, and all the exocyclic substituents point into one direction relative to the mean plane described by the B<sub>3</sub>N<sub>3</sub> core. Six of the dichloroethane solvent molecules are located in layers that alternate with layers consisting of the main molecules **3** (Figure S7, Supporting Information). The remaining two solvent molecules are highly disordered and are positioned in channels that propagate along the crystallographic  $c$  axis. The channels are smaller than the cavity of the individual macrocycles, because the aryl substituents and solvents in layers above and below each macrocycle reach into the channels (Figure 1c).

Compound **3** forms colorless crystals that are blue-emissive when exposed to UV light. In solution, the absorption spectra of **3** show two distinct bands around 420 and 390 nm, independent of the solvent (Figure S8, Supporting Information). These bands are attributed to intramolecular charge transfer (ICT) from triarylamine donor sites ( $n_N/\pi$ -centered orbitals) to triarylborane acceptor sites ( $n_B/\pi^*$ -centered orbitals). Photoexcitation gives rise to an intense emission (CH<sub>2</sub>Cl<sub>2</sub>:  $\lambda_{em} = 460$  nm,  $\Phi = 0.76$ ), which experiences a pronounced red-shift with increasing solvent polarity (Figure 1d and Figure S8, Supporting Information). This solvatochromic effect in the emission, but not the absorption spectra, suggests a more polarized excited state upon ICT, a phenomenon

that is consistent with the formation of a B/N D– $\pi$ –A system.<sup>[7]</sup>

DFT and TDDFT calculations (B3LYP/6-31G\*) were carried out on a simplified derivative (**3<sub>th</sub>**, R = Ph and phenylene  $\pi$ -system in C) in  $D_3$  symmetry (minimization in  $C_3$  symmetry gave slightly higher energy) and the results are summarized along with experimental data in Table 1.<sup>[18]</sup> The HOMO of **3<sub>th</sub>** is degenerate ( $e$ ) with contributions of the nitrogen atoms and the bridging phenylene rings, while the degenerate LUMOs ( $e$ ) are mostly localized on the boron p orbitals with smaller contributions of the exocyclic phenyl rings (Figure 2). The HOMO-2 and LUMO + 2 orbitals are totally symmetric ( $a_2$ ) and thus feature contributions from all of the filled N and empty B p orbitals, respectively. Again, p– $\pi$  delocal-

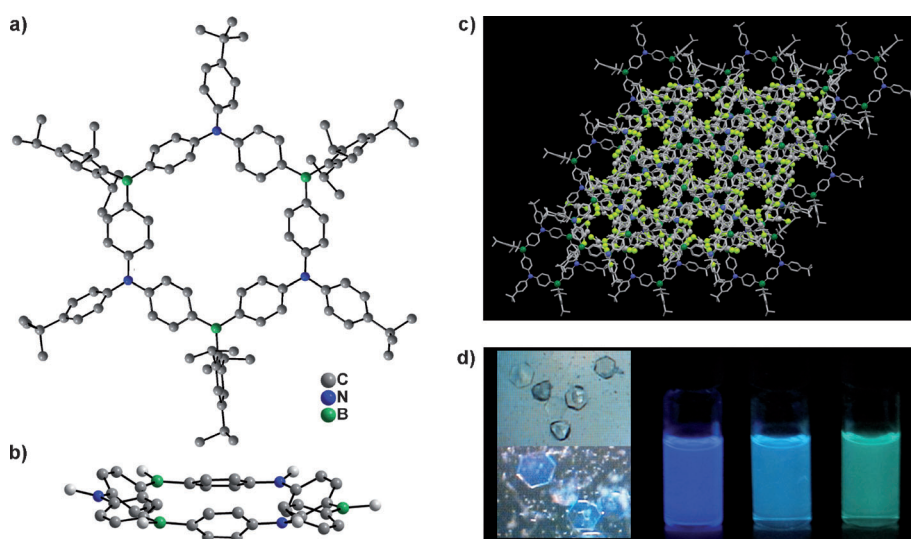


**Figure 1.** a) X-ray structure of **3** (solvents and hydrogen atoms omitted). b) Side view without exocyclic substituents. c) Supramolecular structure of **3** viewed along the crystallographic  $c$  axis (only solvent outside the channels shown; Cl yellow). d) Left: photographs of crystals of **3** without (top) and with (bottom) UV irradiation at 365 nm; photographs of solutions of **3** in (left to right) toluene, CH<sub>2</sub>Cl<sub>2</sub>, and propylene carbonate, irradiated at 365 nm.



**Table 1:** Computational and experimental data for **3**.

Parameter	CV <sup>[a]</sup> [eV]	SWV <sup>[a]</sup> [eV]	DFT <sup>[b]</sup> [eV]	UV/Vis [nm] ([eV])	TD-DFT <sup>[b]</sup> [nm] ([eV])
$E_{\text{LUMO}}$	-2.27	-2.30	-1.69		
$E_{\text{HOMO}}$	-5.26	-5.30	-5.01		
$\Delta E_{\text{gap/UV}}$	2.99	3.00	3.32	420 (2.96)	432 (2.87) <sup>[c]</sup>

[a] Reference: ferrocene at 4.80 eV below vacuum, CV = cyclic voltammetry, SWV = square-wave voltammetry. [b] Computations performed on **3**<sub>th</sub>. [c] Allowed  $S_2 \leftarrow S_0$  transition.

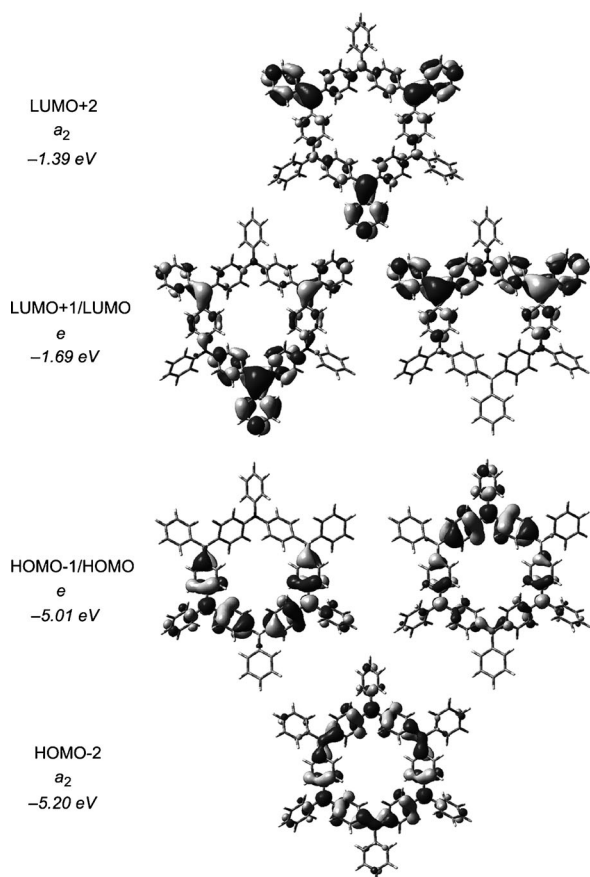


**Figure 2.** Kohn-Sham orbital representation for the ground state frontier orbitals of **3** (B3LYP/6-31G\*).).

alization into the bridging phenylene rings is more pronounced in the N-centered HOMO-2 than the B-centered LUMO + 2. This is in contrast to results for the corresponding hexaaza and hexabora analogues **A**<sub>th</sub> and **B**<sub>th</sub> (R = Ph, phenylene  $\pi$ -system), for which both the HOMO and LUMO show delocalization throughout the ring system.<sup>[16,19]</sup> Based on TDDFT calculations, the  $S_1 \leftarrow S_0$  transition (HOMO-1 to LUMO + 1/HOMO to LUMO) is symmetry forbidden because of cancellation of the transition dipole moments, as is typically observed for highly symmetric macrocycles, including **A** and **B**.<sup>[14,16]</sup> While in solution lower symmetry conformations may be adopted, the structure of the cycle is expected to be quite rigid. The experimentally observed absorption bands are there-

fore assigned to doubly degenerate  $n_N \pi - n_B \pi^*$  transitions to  $S_2$  and  $S_3$ , for which HOMO-2 and LUMO + 2 contributions are mixed in.<sup>[16]</sup>

The electrochemical properties of **3** were examined by cyclic and square wave voltammetry (Figure 3). Three

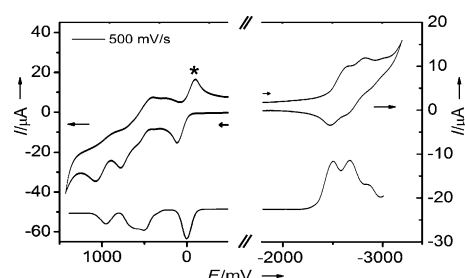


**Figure 3.** Cyclic (top) and square-wave (bottom) voltammograms for **3**; oxidation (left) in  $\text{CH}_2\text{Cl}_2$  and reduction (right) in THF (0.1 M  $[\text{Bu}_4\text{N}][\text{PF}_6]$ ) versus  $\text{Fc}^{0/+}$  ( $\text{Fc} = [(\eta\text{-C}_5\text{H}_5)_2\text{Fe}]$ ) as an internal reference (indicated with an asterisk).

oxidation and three reduction waves were observed. A comparison of the electrochemical data with those reported for the azacyclophane **A** (phenylene  $\pi$ -system)<sup>[11]</sup> and boracyclophane **B** (fluorene  $\pi$ -system)<sup>[14]</sup> provides insights into the mutual electronic effects of the adjacent boron and nitrogen centers in the ambipolar structure of **3** (Table 2). Relative to the azacyclophane **A**, **3** is oxidized at more positive potentials, because the presence of the electron-deficient neighboring boron atoms decreases the electron density at nitrogen. Conversely, more negative potentials are needed to reduce the boron sites in **3** compared with the boracyclophane **B**, because of an increase in the electron density at boron in the presence of the neighboring amine groups. These experimental findings suggest that the HOMO level is lowered, while the LUMO is elevated. We also note that the potentials for reduction of **3** are similar to the last three reduction steps in **B**, while the potentials for oxidation are similar to the last three oxidation steps in **A**, indicating that the electronic effect of a reduced borane moiety is comparable to that of a neutral amine and the effect of an oxidized amine to that of a neutral borane, respectively. Importantly, despite the relatively higher LUMO than in **A** and the relatively lower HOMO than in **B**, theoretical calculations reveal that the HOMO-LUMO gap in the ambipolar species **3** is the smallest among these macrocycles, which is consistent with the relatively small optical gap of 2.96 eV determined by UV/Vis spectroscopy.<sup>[20]</sup>

**Table 2:** cyclic voltammetry data for **3** and of **A** and **B** (vs  $\text{Fc}^{0/+}$ ,  $\nu = 100 \text{ mVs}^{-1}$ ).

Species	Event	$E^1_{1/2}$	$E^2_{1/2}$	$E^3_{1/2}$	$E^4_{1/2}$	$E^5_{1/2}$	$E^6_{1/2}$
<b>A</b> <sup>[a]</sup>	$\text{Ox}^{[c]}$	-0.28	-0.17	+0.20	+0.45	+0.72 <sup>[f]</sup>	+0.72 <sup>[f]</sup>
	$\text{Ox}^{[d]}$				+0.46 <sup>[e]</sup>	+0.65 <sup>[e]</sup>	+0.94 <sup>[e]</sup>
	Red <sup>[e]</sup>				-2.53	-2.72	-2.84 <sup>[e]</sup>
<b>B</b> <sup>[b]</sup>	Red <sup>[e]</sup>	-2.10 <sup>[b]</sup>	-2.10 <sup>[b]</sup>	-2.27	-2.44	-2.57	-2.70

[a] From Ref. [11]. [b] From Ref. [14]. [c] 0.1 M  $[\text{Bu}_4\text{N}][\text{BF}_4]$  in  $\text{CH}_2\text{Cl}_2$ . [d] 0.1 M  $[\text{Bu}_4\text{N}][\text{PF}_6]$  in  $\text{CH}_2\text{Cl}_2$ . [e] 0.1 M  $[\text{Bu}_4\text{N}][\text{PF}_6]$  in THF. [f] Overlapping. [g] Determined by SWV.



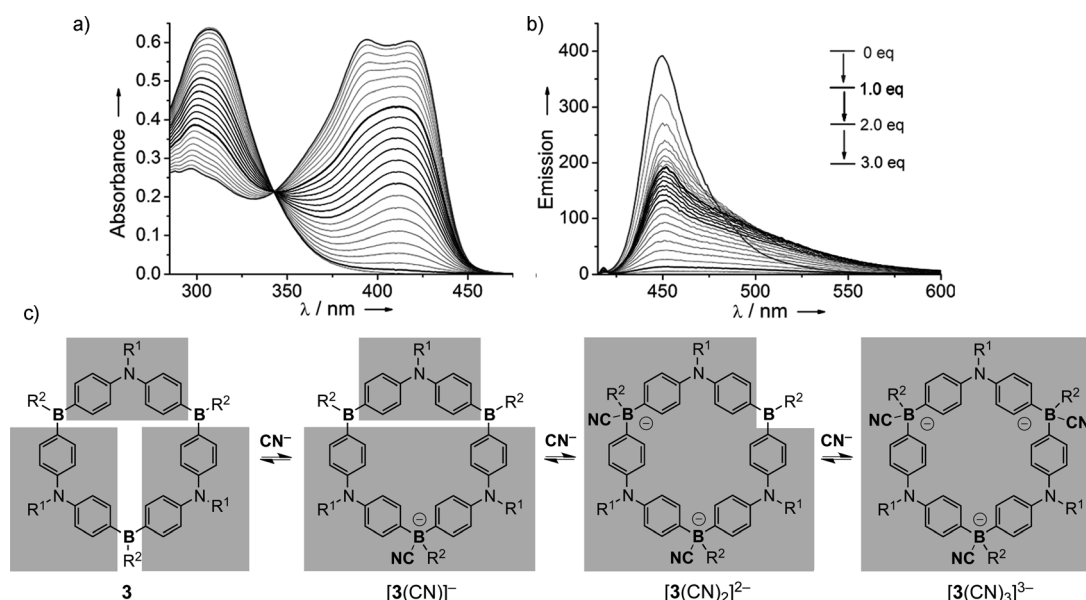


**Figure 4.** Titration of **3** with  $[n\text{Bu}_4\text{N}]\text{CN}$  in toluene monitored by a) UV/Vis and b) fluorescence spectroscopy ( $[\mathbf{3}]^0 = 1.429 \times 10^{-5} \text{ M}$ ;  $[\text{CN}^-] = 1.042 \times 10^{-3} \text{ M}$ ,  $\lambda_{\text{ex}} = 419 \text{ nm}$ ). c) Illustration of electron-donor segments for **3** and the corresponding anion complexes.

The presence of electron-deficient organoborane moieties also suggests possible use of these molecules in the recognition of anions.<sup>[21]</sup> The anion binding behavior was evaluated by titration experiments with the cyanide anion. As shown in Figure 4, stepwise addition of  $[n\text{Bu}_4\text{N}]\text{CN}$  to a solution of **3** in toluene resulted in a gradual decrease in the UV absorbance and emission intensity. Three distinct regimes were observed, consistent with addition of the anion to the three available borane moieties, albeit with little or no cooperative effects<sup>[22,23]</sup> ( $\lg\beta_{11} \approx 8.0$ ,  $\lg\beta_{12} = 15.7$ ,  $\lg\beta_{13} = 23.0$ ). Noteworthy is that, although the absorption wavelength does not change dramatically, in the emission spectra a clear bathochromic tailing is observed, which we attribute to new charge transfer (CT) pathways upon generation of an electron-rich organoborate site (Figure 4c; see also Ref. [8,24]). A comparison to the quenching behavior of the boracyclopentane **B** provides further insights. In the case of **B**, only slightly more than 1 equivalent of quencher is needed to completely turn off the emission of the host.<sup>[14]</sup> In contrast, to fully quench the fluorescence of **3**, more than 3 equivalents of  $\text{CN}^-$  are required, corresponding to full complexation of all three Lewis acidic B centers. This suggests that emission from CT states in the partially complexed species  $[\mathbf{3}(\text{CN})]^-$  and  $[\mathbf{3}(\text{CN})_2]^{2-}$  remains strong, whereas a very weakly emissive low-energy CT state is generated upon anion binding in  $[\mathbf{B}(\text{CN})]^-$ . This CT state is believed to serve as an energy trap, resulting in effective quenching of the emission.<sup>[14]</sup>

In conclusion, the synthesis of the first ambipolar  $\pi$ -conjugated B–N macrocycle was accomplished by cyclization of the corresponding linear oligomer under pseudo-high dilution conditions. As confirmed by single-crystal X-ray diffraction, N donor and B acceptor sites are alternating in the highly symmetric ring system of **3**. The D– $\pi$ –A type arrangement results in mutual interactions between B and N as is evidenced by electrochemical measurements and reflected in

a pronounced solvatochromic effect on the emission. Macrocycles, such as **3**, combine aspects of electron-rich aza- and electron-deficient boracyclopentanes suggesting possible applications as ambipolar semiconductor materials. The strong luminescence in solution also lends itself to use in anion recognition and our studies indicate that, in the presence of low levels of cyanide, fluorescence results from emissive charge-transfer states, which is in stark contrast to the respective boracyclopentane **B**.

Received: May 16, 2012

Published online: July 5, 2012

**Keywords:** ambipolar · anion recognition · luminescence · macrocycle · organoborane

- [1] a) E. P. A. Stock, *Ber. Dtsch. Chem. Ges.* **1926**, 59, 2210; b) P. v. R. Schleyer, H. Jiao, N. J. R. v. Eikema Hommes, V. G. Malkin, O. L. Malkina, *J. Am. Chem. Soc.* **1997**, 119, 12669.
- [2] a) K. Ma, M. Scheibitz, S. Scholz, M. Wagner, *J. Organomet. Chem.* **2002**, 652, 11; b) Z. Q. Liu, T. B. Marder, *Angew. Chem.* **2008**, 120, 248; *Angew. Chem. Int. Ed.* **2008**, 47, 242; c) M. J. D. Bosdet, W. E. Piers, *Can. J. Chem.* **2009**, 87, 8; T. B. Marder, *Angew. Chem.* **2007**, 119, 8262; *Angew. Chem. Int. Ed.* **2007**, 46, 8116; d) E. R. Abbey, L. N. Zakharov, S. Y. Liu, *J. Am. Chem. Soc.* **2011**, 133, 11508.
- [3] a) A. N. Lamm, E. B. Garner, D. A. Dixon, S. Y. Liu, *Angew. Chem.* **2010**, 122, 8333; *Angew. Chem. Int. Ed.* **2010**, 49, 8157; b) P. G. Campbell, L. N. Zakharov, D. J. Grant, D. A. Dixon, S. Y. Liu, *J. Am. Chem. Soc.* **2010**, 132, 3289.
- [4] a) C. A. Jaska, D. J. H. Emslie, M. J. D. Bosdet, W. E. Piers, T. S. Sorensen, M. Parvez, *J. Am. Chem. Soc.* **2006**, 128, 10885; b) M. J. D. Bosdet, W. E. Piers, T. S. Sorensen, M. Parvez, *Angew. Chem.* **2007**, 119, 5028; *Angew. Chem. Int. Ed.* **2007**, 46, 4940.
- [5] E. R. Abbey, L. N. Zakharov, S. Y. Liu, *J. Am. Chem. Soc.* **2010**, 132, 16340.



- [6] Borazines have also been utilized as scaffolds for attachment of conjugated aromatic groups: A. Wakamiya, T. Ide, S. Yamaguchi, *J. Am. Chem. Soc.* **2005**, *127*, 14859.
- [7] a) Z. Yuan, J. C. Collings, N. J. Taylor, T. B. Marder, C. Jardin, J.-F. Halet, *J. Solid State Chem.* **2000**, *154*, 5; b) C. D. Entwistle, T. B. Marder, *Chem. Mater.* **2004**, *16*, 4574; c) Y. Shiota, *J. Mater. Chem.* **2005**, *15*, 75; d) X. Y. Liu, D. R. Bai, S. N. Wang, *Angew. Chem.* **2006**, *118*, 5601; *Angew. Chem. Int. Ed.* **2006**, *45*, 5475; e) F. Li, W. Jia, S. Wang, Y. Zhao, Z.-H. Lu, *J. Appl. Phys.* **2008**, *103*, 034509; f) J. C. Collings, S. Y. Poon, C. Le Droumaguet, M. Charlot, C. Katan, L. O. Palsson, A. Beeby, J. A. Mosely, H. M. Kaiser, D. Kaufmann, W. Y. Wong, M. Blanchard-Desce, T. B. Marder, *Chem. Eur. J.* **2009**, *15*, 198; g) R. Stahl, C. Lambert, C. Kaiser, R. Wortmann, R. Jakober, *Chem. Eur. J.* **2006**, *12*, 2358; h) A. Proñ, M. Baumgarten, K. Müllen, *Org. Lett.* **2010**, *12*, 4236; i) L. Weber, D. Eickhoff, T. B. Marder, M. A. Fox, P. J. Low, A. D. Dwyer, D. J. Tozer, S. Schwedler, A. Brockhinke, H.-G. Stämmler, B. Neumann, *Chem. Eur. J.* **2012**, *18*, 1369.
- [8] H. C. Schmidt, L. G. Reuter, J. Hamacek, O. S. Wenger, *J. Org. Chem.* **2011**, *76*, 9081.
- [9] a) M. Iyoda, *Pure Appl. Chem.* **2010**, *82*, 831; b) A. Mishra, C.-Q. Ma, P. Bäuerle, *Chem. Rev.* **2009**, *109*, 1141; c) W. Zhang, J. S. Moore, *Angew. Chem.* **2006**, *118*, 4524; *Angew. Chem. Int. Ed.* **2006**, *45*, 4416; d) S. Höger, *Chem. Eur. J.* **2004**, *10*, 1320; e) C. Grave, A. D. Schlüter, *Eur. J. Org. Chem.* **2002**, 3075.
- [10] a) L. Zang, Y. Che, J. S. Moore, *Acc. Chem. Res.* **2008**, *41*, 1596; b) C. S. Hartley, J. S. Moore, *J. Am. Chem. Soc.* **2007**, *129*, 11682.
- [11] A. Ito, Y. Yokoyama, R. Aihara, K. Fukui, S. Eguchi, K. Shizu, T. Sato, K. Tanaka, *Angew. Chem.* **2010**, *122*, 8381; *Angew. Chem. Int. Ed.* **2010**, *49*, 8205.
- [12] Examples: a) P. Jutzi, N. Lenze, B. Neumann, H.-G. Stämmler, *Angew. Chem.* **2001**, *113*, 1469; *Angew. Chem. Int. Ed.* **2001**, *40*, 1423; b) T. J. Wedge, M. F. Hawthorne, *Coord. Chem. Rev.* **2003**, *240*, 111; c) M. A. Fox, J. A. K. Howard, J. A. H. MacBride, A. Mackinnon, K. Wade, *J. Organomet. Chem.* **2003**, *680*, 155; d) M. Scheibitz, R. F. Winter, M. Bolte, H. W. Lerner, M. Wagner, *Angew. Chem.* **2003**, *115*, 954; *Angew. Chem. Int. Ed.* **2003**, *42*, 924; e) H.-Y. Gong, X.-H. Zhang, D.-X. Wang, H.-W. Ma, Q.-Y. Zheng, M.-X. Wang, *Chem. Eur. J.* **2006**, *12*, 9262; f) K. Venkatasubbaiah, T. Pakkirisamy, R. A. Lalancette, F. Jäkle, *Dalton Trans.* **2008**, 4507; g) E.-X. Zhang, D.-X. Wang, Q.-Y. Zheng, M.-X. Wang, *Org. Lett.* **2008**, *10*, 2565; h) D. E. Herbert, J. B. Gilroy, W. Y. Chan, L. Chabanne, A. Staubitz, A. J. Lough, I. Manners, *J. Am. Chem. Soc.* **2009**, *131*, 14958.
- [13] F. P. Gabbaï, *Angew. Chem.* **2003**, *115*, 2318; *Angew. Chem. Int. Ed.* **2003**, *42*, 2218.
- [14] P. Chen, F. Jäkle, *J. Am. Chem. Soc.* **2011**, *133*, 20142.
- [15] a) Y. Qin, I. Kiburu, S. Shah, F. Jäkle, *Macromolecules* **2006**, *39*, 9041; b) P. Chen, R. A. Lalancette, F. Jäkle, *J. Am. Chem. Soc.* **2011**, *133*, 8802.
- [16] See the Supporting Information for further details.
- [17] Crystal data for **3** (CCDC 882152 contains the supplementary crystallographic data for this paper. These data can be obtained free of charge from The Cambridge Crystallographic Data Centre via [www.ccdc.cam.ac.uk/data\\_request/cif](http://www.ccdc.cam.ac.uk/data_request/cif)):  $C_{111}H_{132}B_3N_3 \times 6 C_2H_4Cl_2$ ,  $M_r = 2134.34$ , colorless hexagon,  $0.51 \times 0.47 \times 0.17 \text{ mm}^3$ , rhombohedral space group  $R\bar{3}$ ,  $a = b = 21.3886(11) \text{ \AA}$ ,  $c = 46.765(3) \text{ \AA}$ ,  $V = 18528(2) \text{ \AA}^3$ ,  $Z = 6$ ,  $\rho_{\text{calcd}} = 1.148 \text{ g cm}^{-3}$ ,  $\mu = 2.807 \text{ mm}^{-1}$ ,  $F(000) = 6804$ ,  $T = 100(2) \text{ K}$ ,  $R1 = 0.129$ ,  $wR2 = 0.383$ , 7564 independent reflections  $[2.57 - 71.8^\circ]$  and 433 parameters. Two additional disordered solvent molecules per main molecule were located in the channels and removed using the squeeze routine in the program Platon (A. L. Spek, *J. Appl. Crystallogr.* **2003**, *36*, 7).
- [18] M. J. Frisch, et al. Gaussian 03, revision C.02; Gaussian Inc.: Wallingford, CT, **2004** (see the Supporting Information for a full citation).
- [19] GIAO calculations suggest less aromatic character for **3** in comparison to the corresponding hexabora and hexaaza species (see Table S4, Supporting Information).
- [20] This trend applies to both the formally forbidden  $S_1 \leftarrow S_0$  and the  $S_2 \leftarrow S_0$  transition (see Table S6).
- [21] a) C. R. Wade, A. E. J. Broomsgrove, S. Aldridge, F. P. Gabbaï, *Chem. Rev.* **2010**, *110*, 3958; b) Z. M. Hudson, S. Wang, *Acc. Chem. Res.* **2009**, *42*, 1584.
- [22] A. Sundararaman, K. Venkatasubbaiah, M. Victor, L. N. Zakharov, A. L. Rheingold, F. Jäkle, *J. Am. Chem. Soc.* **2006**, *128*, 16554, and Ref. [8].
- [23] The large value of the binding constants limits the accuracy of the measurement and  $\beta_{11}$  had to be fixed to refine  $\beta_{12}$  and  $\beta_{13}$ . Nevertheless, the relative magnitude of the binding constants for the three processes should be quite accurate and is consistent with a lack of cooperativity.
- [24] a) H. Li, F. Jäkle, *Macromol. Rapid Commun.* **2010**, *31*, 915; b) S.-B. Zhao, P. Wucher, Z. M. Hudson, T. M. McCormick, X.-Y. Liu, S. Wang, X.-D. Feng, Z.-H. Lu, *Organometallics* **2008**, *27*, 6446; c) G. Zhou, M. Baumgarten, K. Müllen, *J. Am. Chem. Soc.* **2008**, *130*, 12477.